Supplementary Materials

A Dual Fluorometric and Colorimetric Sulfide Sensor Based on Coordinating Self-Assembled Nanorods: Applicable for Monitoring Meat Spoilage

Rana Dalapati, Matthew Hunter and Ling Zang *

Department of Materials Science and Engineering, Nano Institute of Utah, University of Utah, Salt Lake City, UT 84112, USA
*Correspondence: lzang@eng.utah.edu

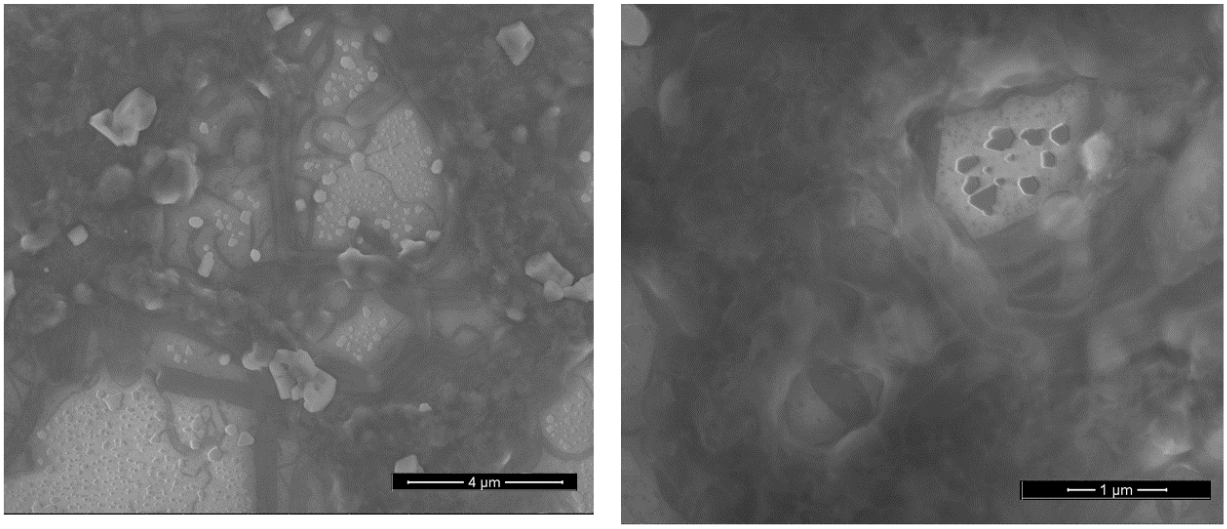

Figure S1. SEM image of the APBI-K.

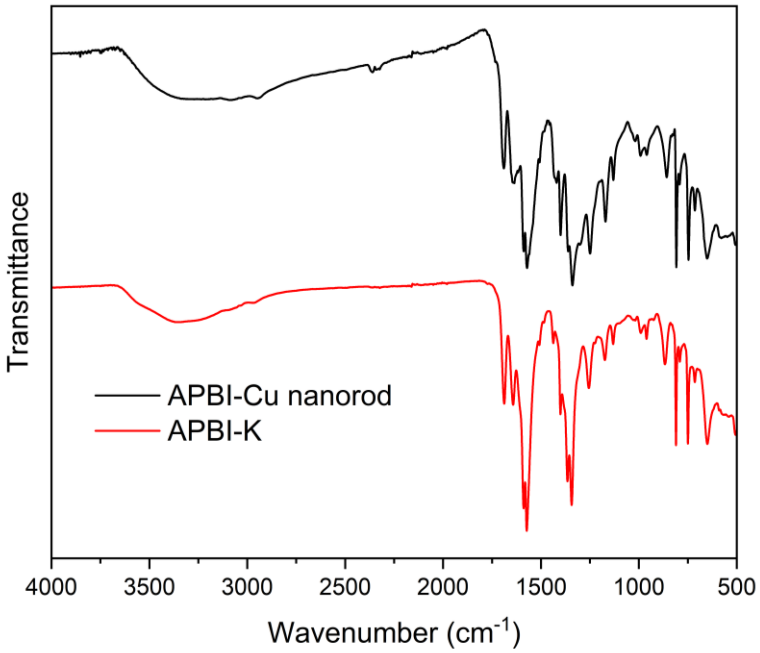

Figure S2. ATR-IR spectra of **APBI-K** and **APBI-Cu** nanorods.

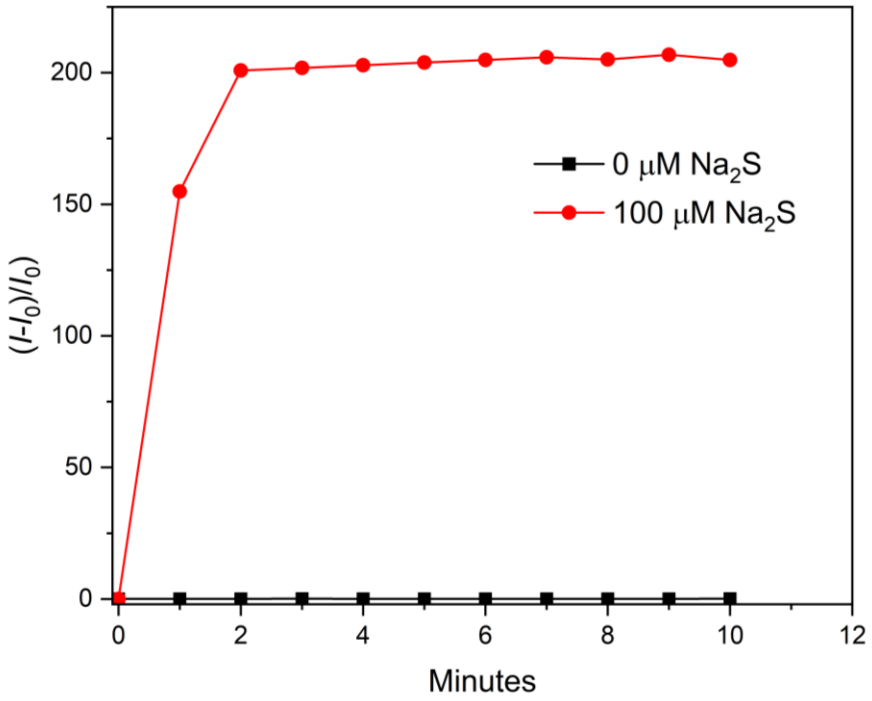

Figure S3. Time dependent relative changes of emission intensity of **APBI-Cu** nanorods with Na_2S.

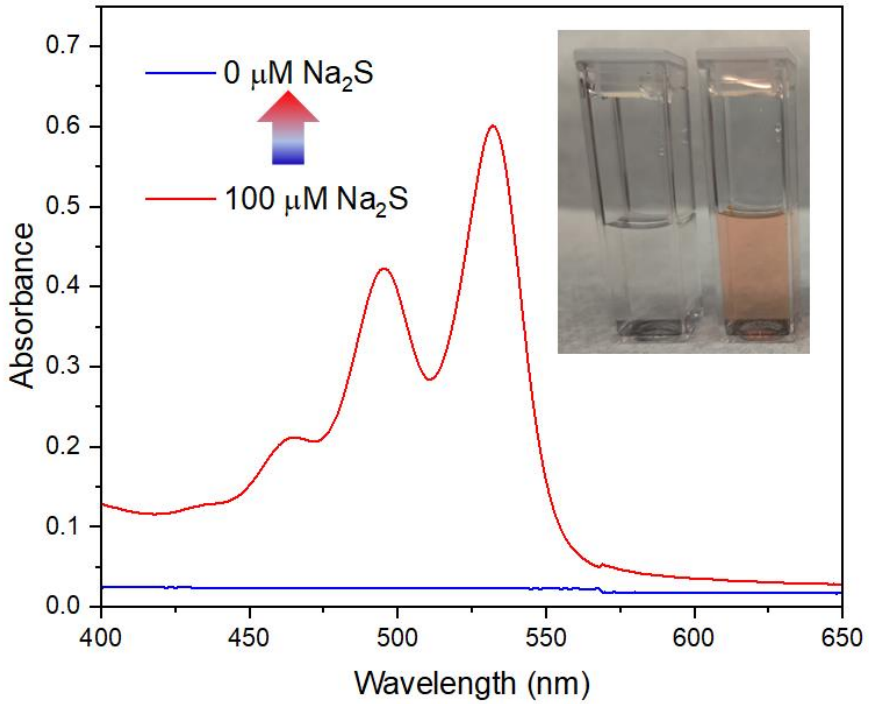

Figure S4. Change in absorption spectra of **APBI-Cu** nanorods in presence of Na_2S. Inset showing corresponding change in color of the solution.

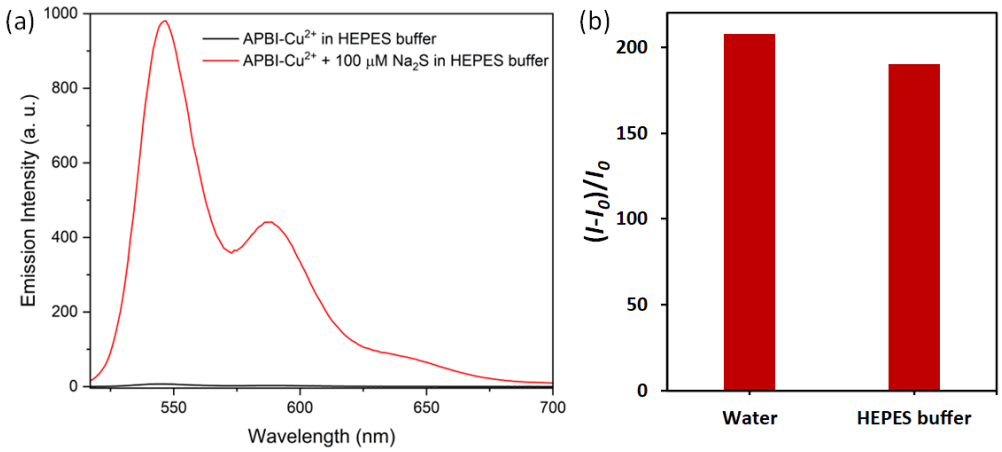

Figure S5. (a) Change in emission spectra of **APBI-Cu** nanorods in presence of Na_2S in HEPES buffer medium at pH 7.4. and other competitive molecules and anions. (b) The bar plot showing the relative change in emission spectra of **APBI-Cu** nanorods in presence of Na_2S in pure water and HEPES buffer medium.

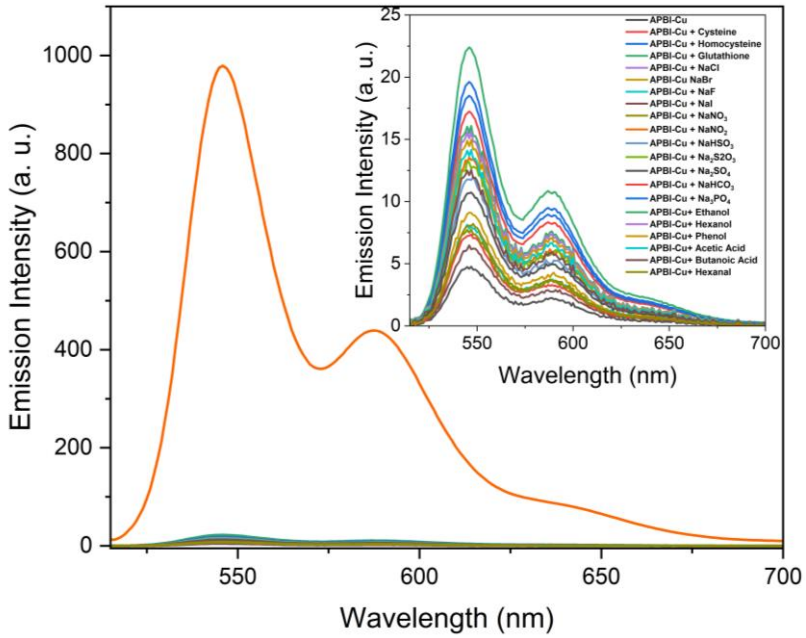

Figure S6. Change in emission spectra of **APBI-Cu** nanorods in presence of Na_2S and other competitive molecules and anions. Inset showing the enlarged view of the spectral change for other analytes.

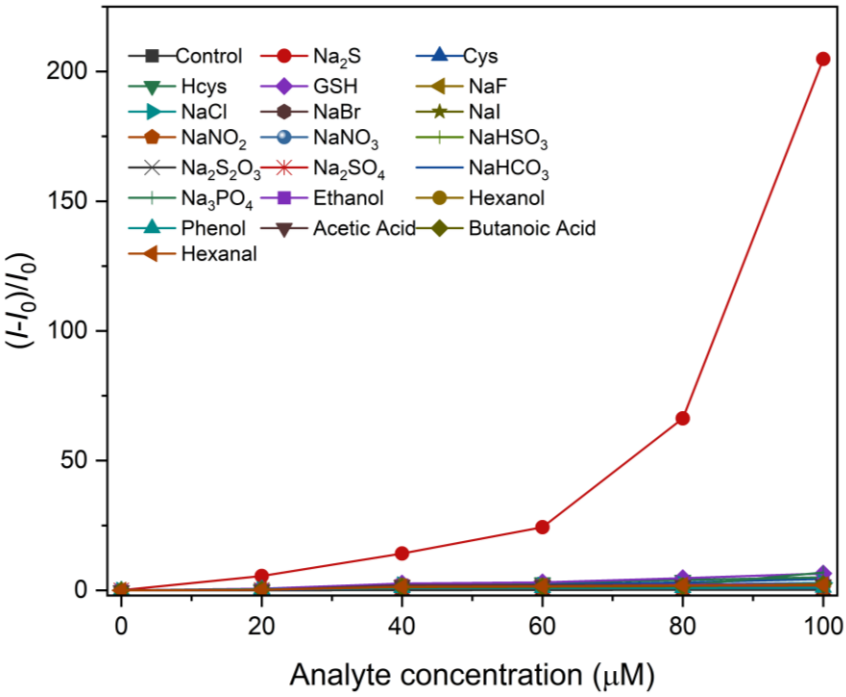

Figure S7: Concentration dependent change in emission spectra of **APBI-Cu** nanorods in presence of Na_2S and other competitive analytes (final concentration: 100 μM).

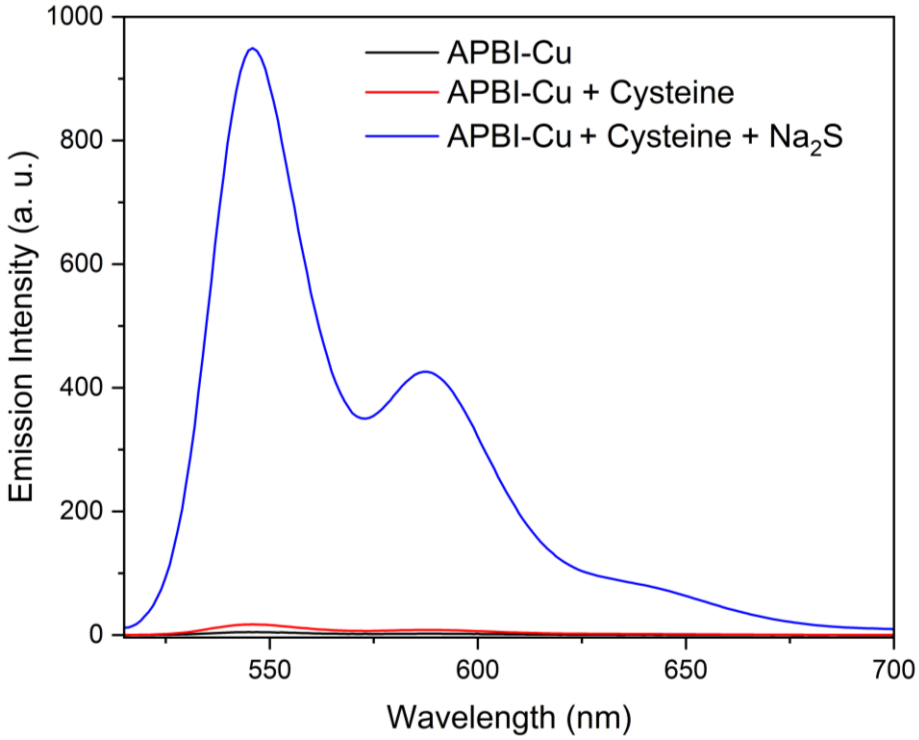

Figure S8: Competitive detection of Na_2S by **APBI-Cu** nanorods in presence of Cysteine.

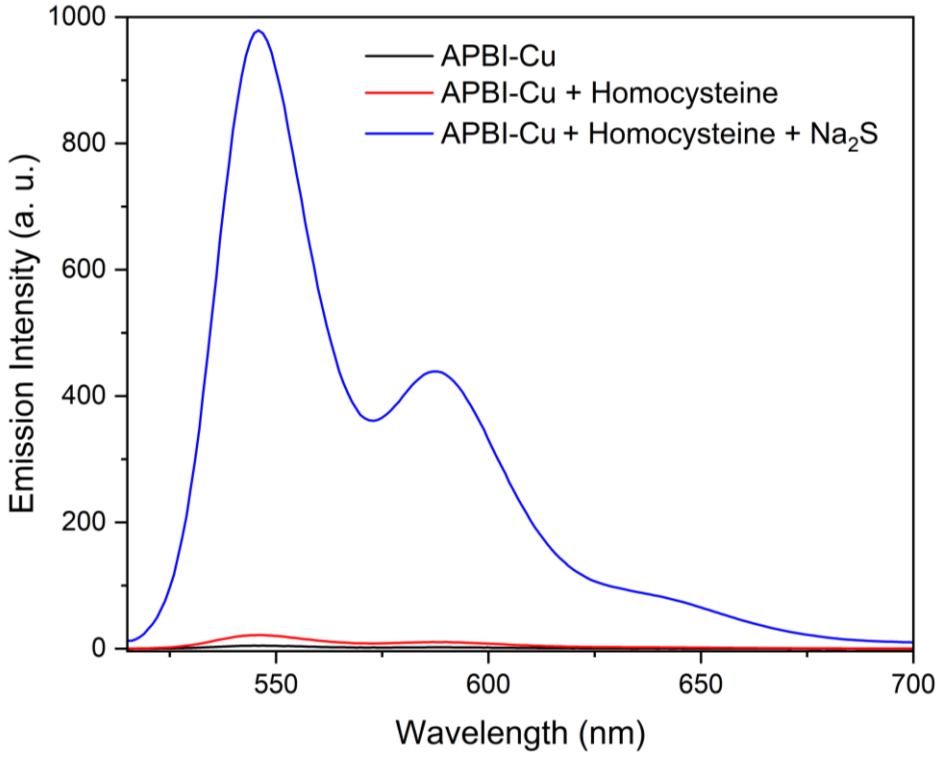

Figure S9: Competitive detection of Na_2S by **APBI-Cu** nanorods in presence of Homocysteine.

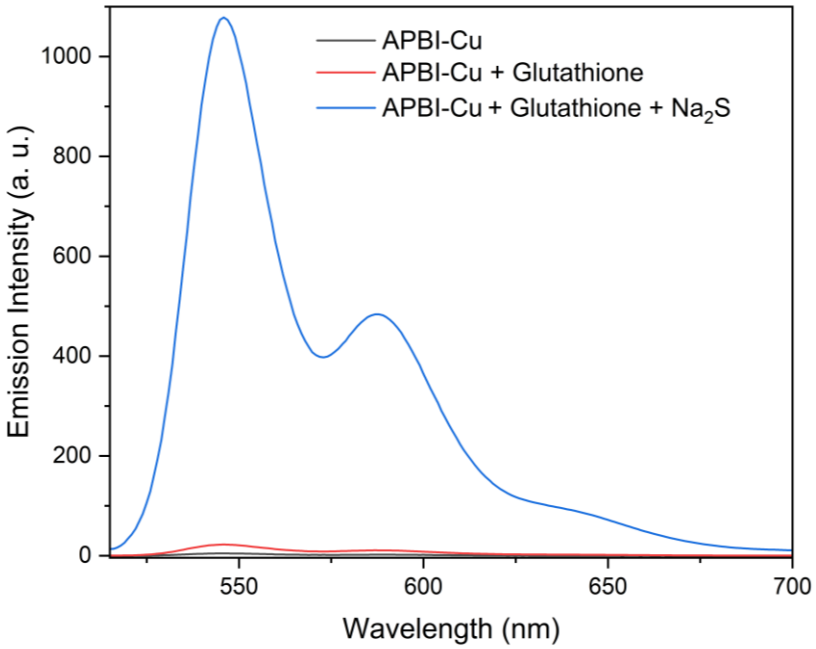

Figure S10: Competitive detection of Na_2S by **APBI-Cu** nanorods in presence of Glutathione.

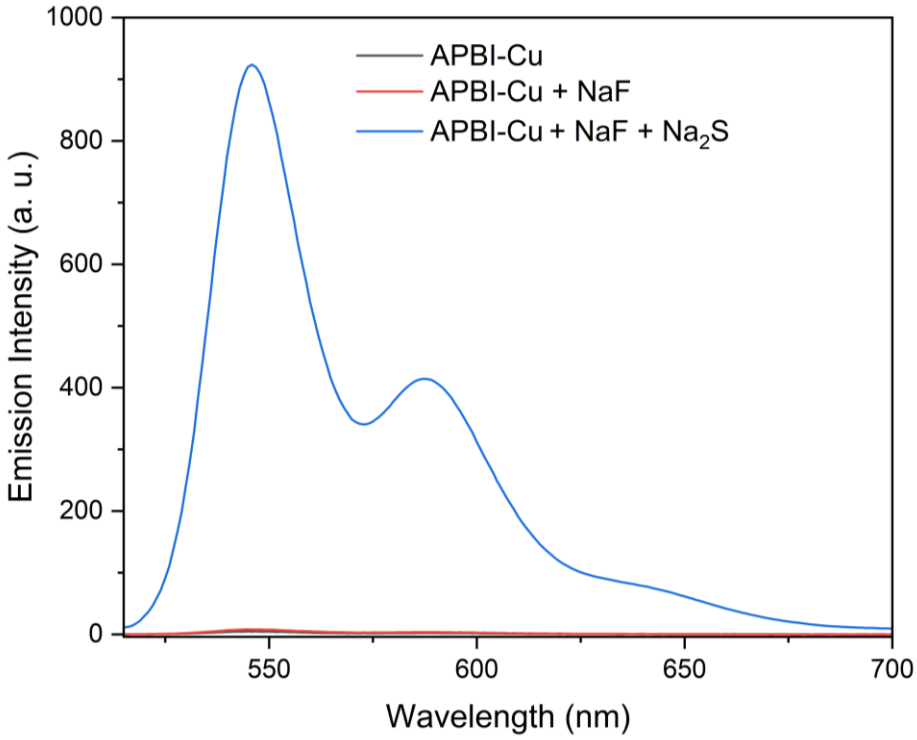

Figure S11: Competitive detection of Na_2S by **APBI-Cu** nanorods in presence of NaF.

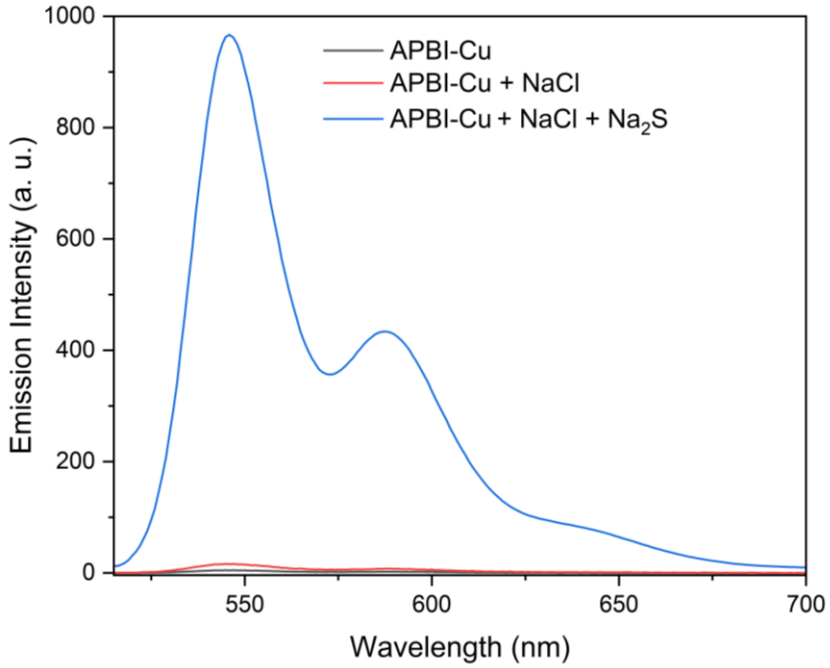

Figure S12: Competitive detection of Na_2S by **APBI-Cu** nanorods in presence of NaCl.

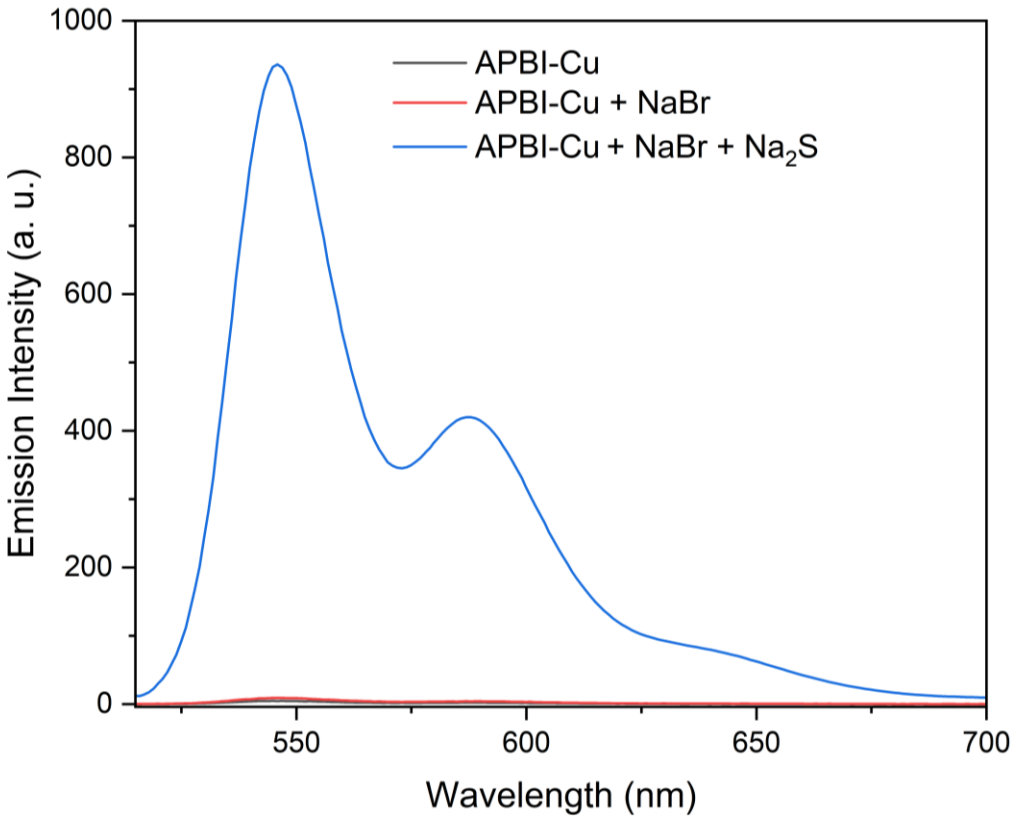

Figure S13: Competitive detection of Na_2S by **APBI-Cu** nanorods in presence of NaBr.

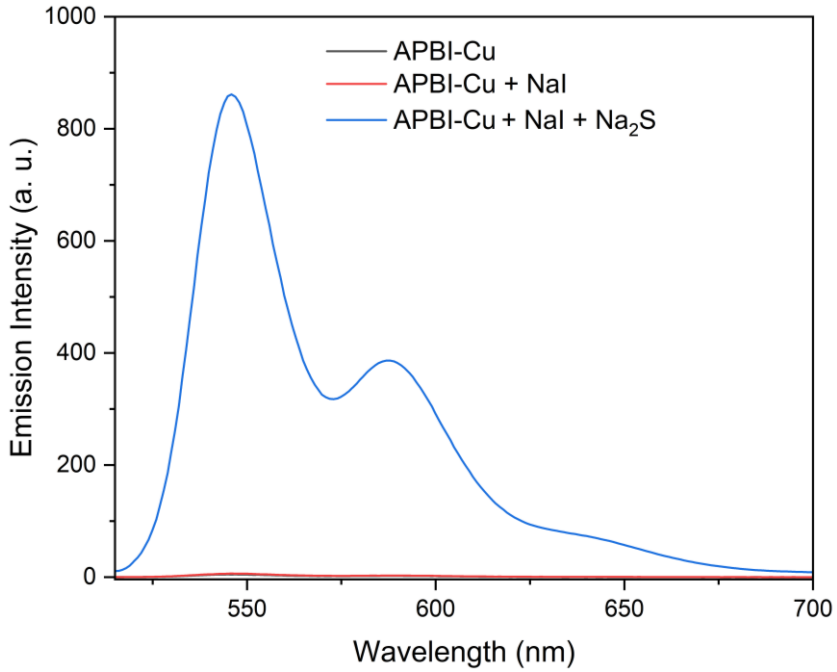

Figure S14: Competitive detection of Na_2S by **APBI-Cu** nanorods in presence of NaI.

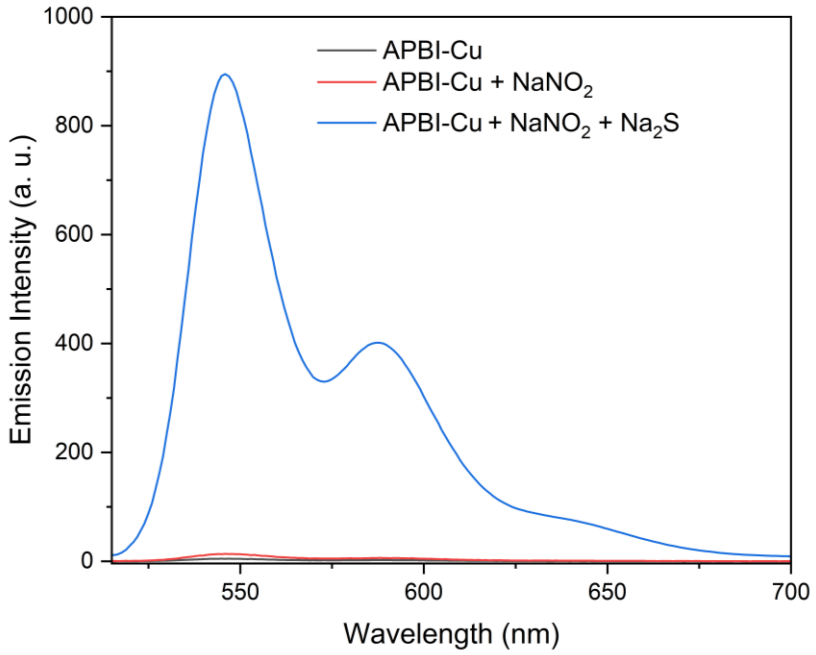

Figure S15: Competitive detection of Na_2S by **APBI-Cu** nanorods in presence of $NaNO_2$.

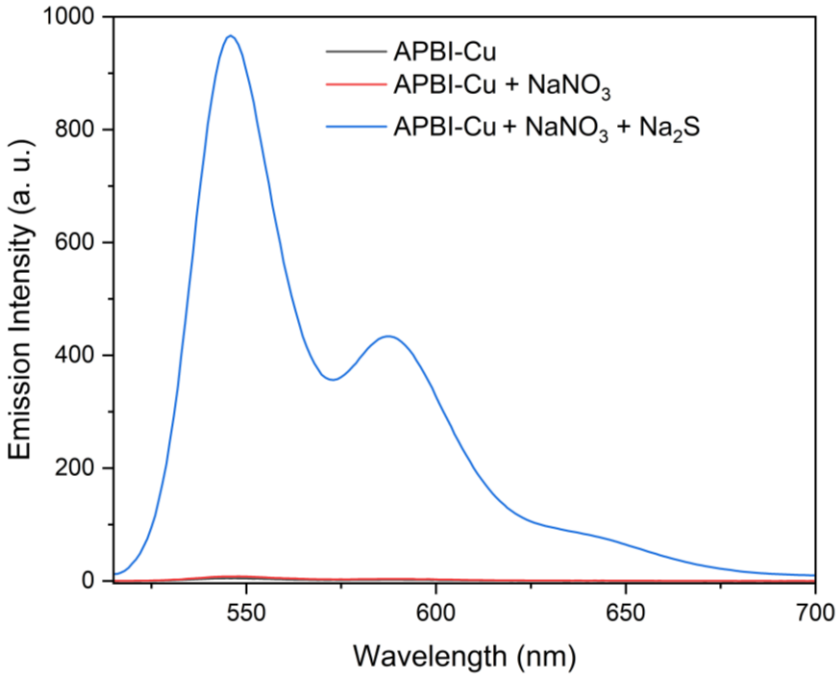

Figure S16: Competitive detection of Na_2S by **APBI-Cu** nanorods in presence of $NaNO_3$.

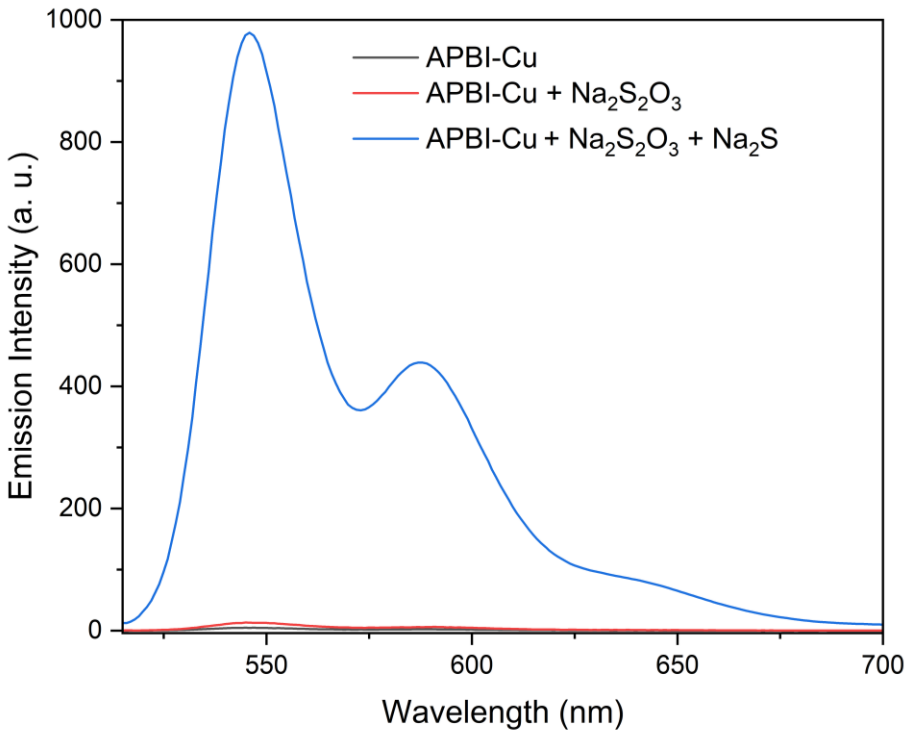

Figure S17: Competitive detection of Na_2S by **APBI-Cu** nanorods in presence of NaS_2O_3.

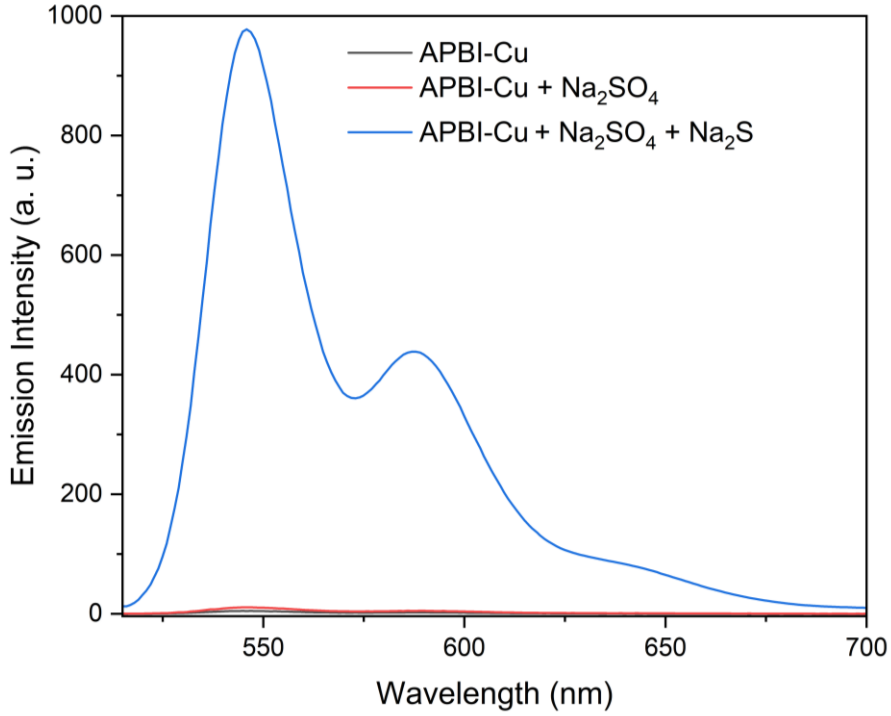

Figure S18: Competitive detection of Na_2S by **APBI-Cu** nanorods in presence of $NaSO_4$.

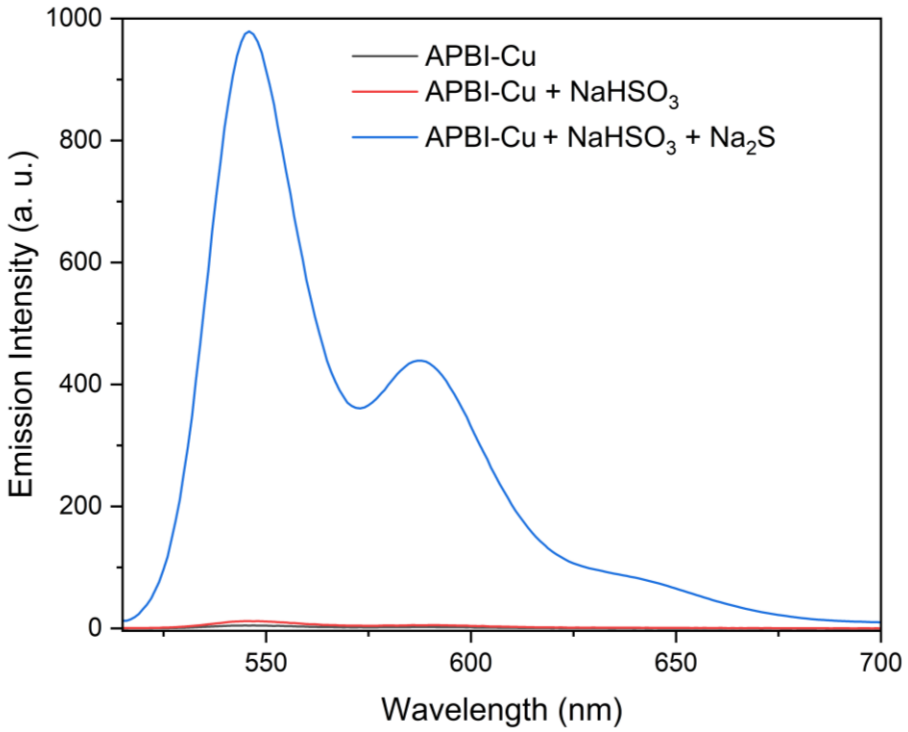

Figure S19: Competitive detection of Na_2S by **APBI-Cu** nanorods in presence of $NaHSO_3$.

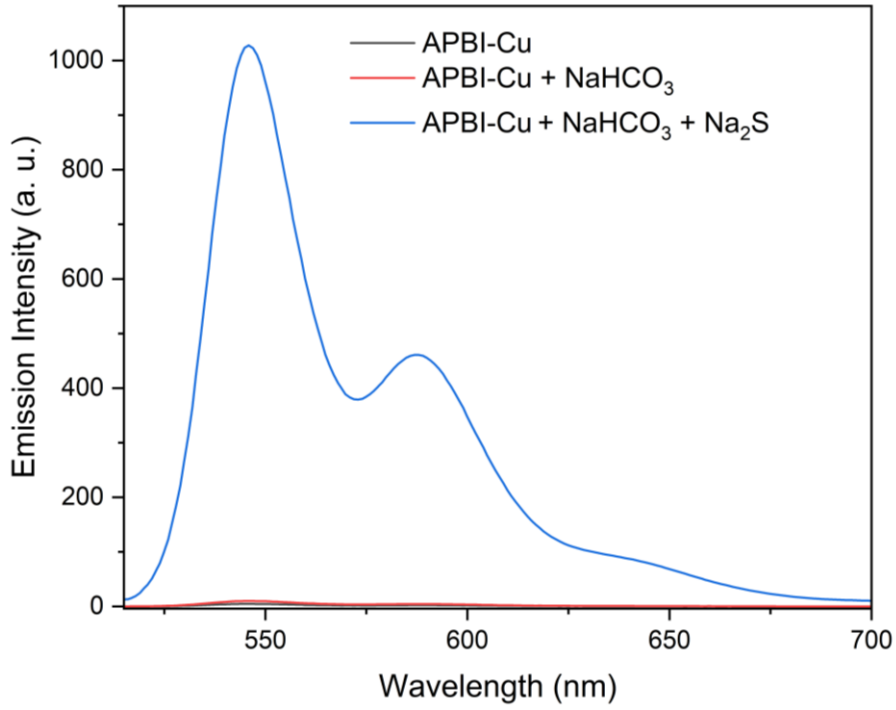

Figure S20: Competitive detection of Na_2S by **APBI-Cu** nanorods in presence of $NaHCO_3$.

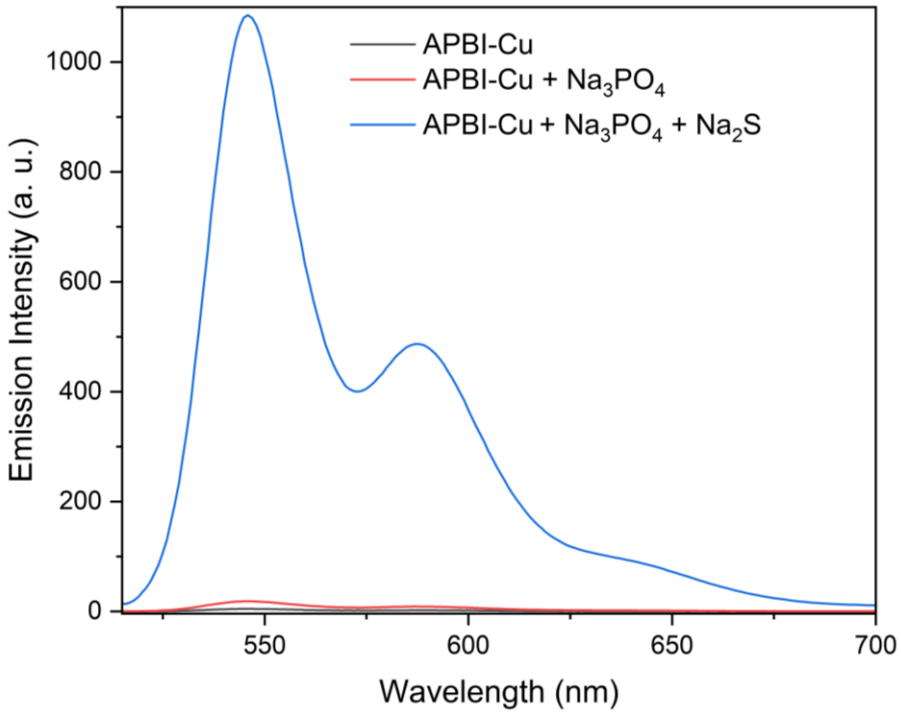

Figure S21: Competitive detection of Na_2S by **APBI-Cu** nanorods in presence of Na_3PO_4.

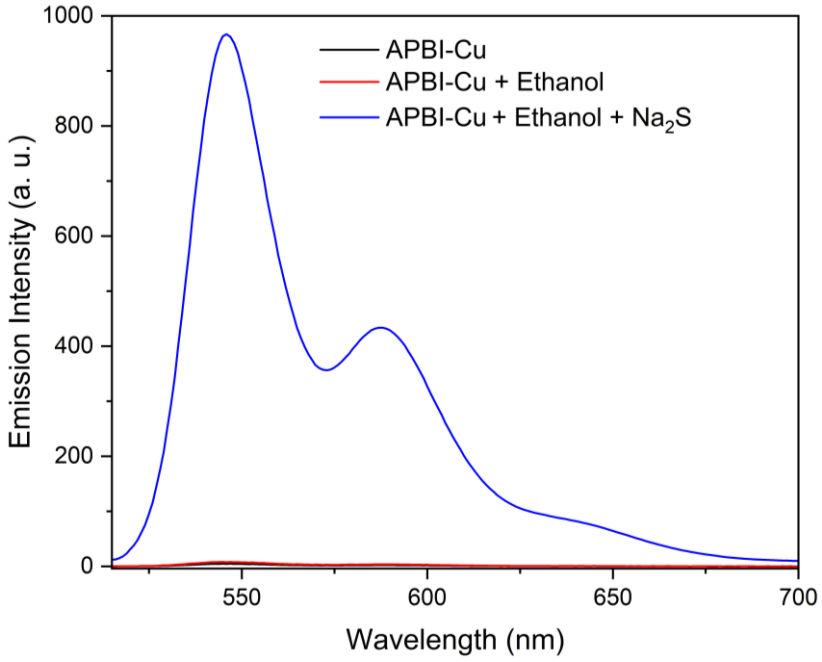

Figure S22: Competitive detection of Na_2S by **APBI-Cu** nanorods in presence of Ethanol.

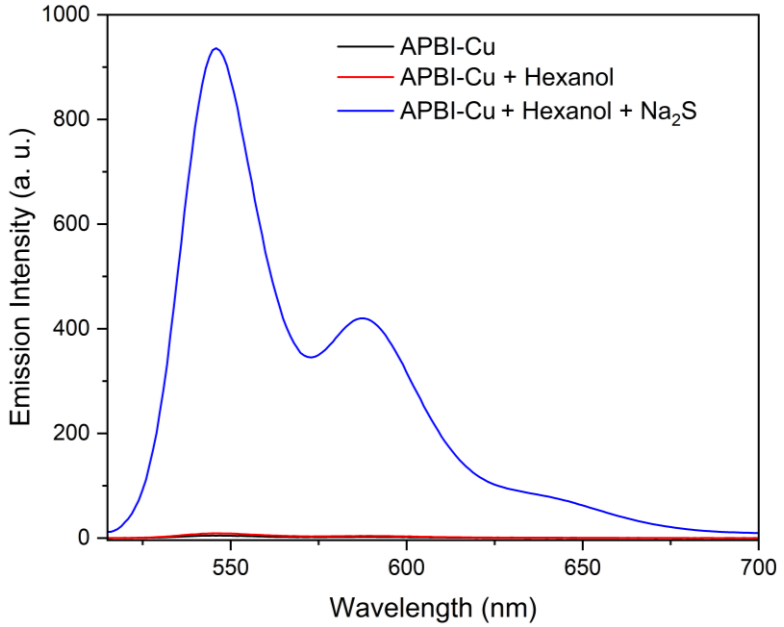

Figure S23: Competitive detection of Na_2S by **APBI-Cu** nanorods in presence of Hexanol.

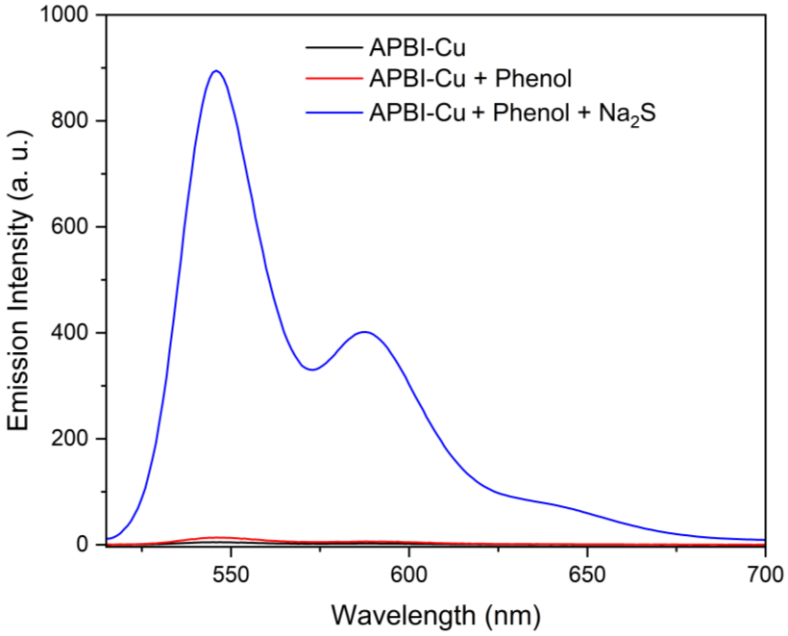

Figure S24: Competitive detection of Na_2S by **APBI-Cu** nanorods in presence of Phenol.

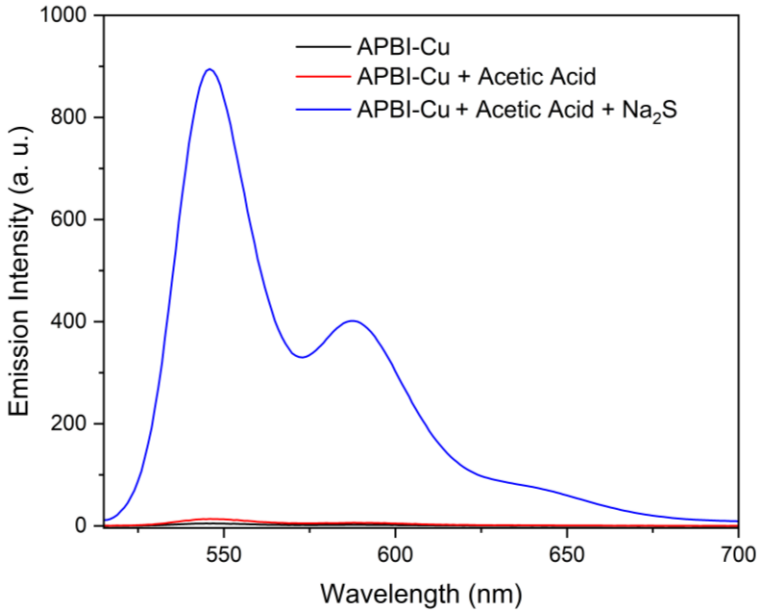

Figure S25: Competitive detection of Na_2S by **APBI-Cu** nanorods in presence of Acetic Acid.

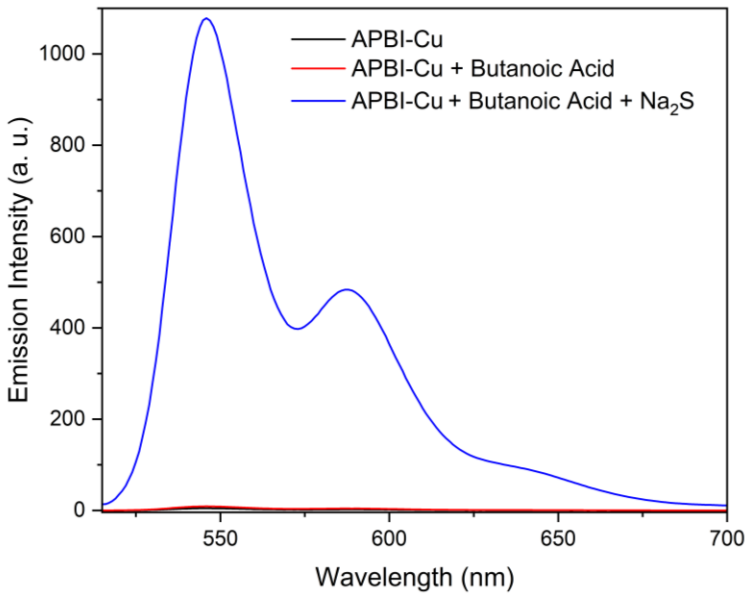

Figure S26: Competitive detection of Na_2S by **APBI-Cu** nanorods in presence of Butanoic Acid.

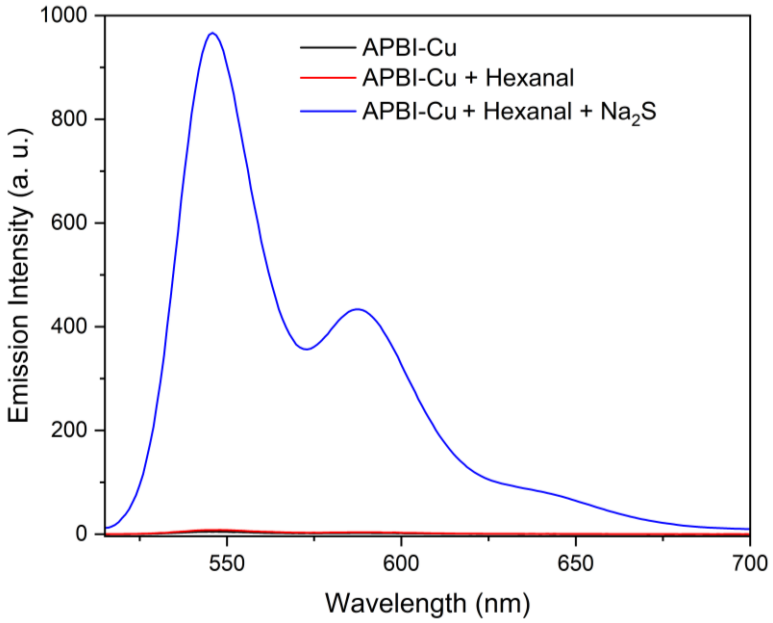

Figure S27: Competitive detection of Na_2S by **APBI-Cu** nanorods in presence of Hexanal.

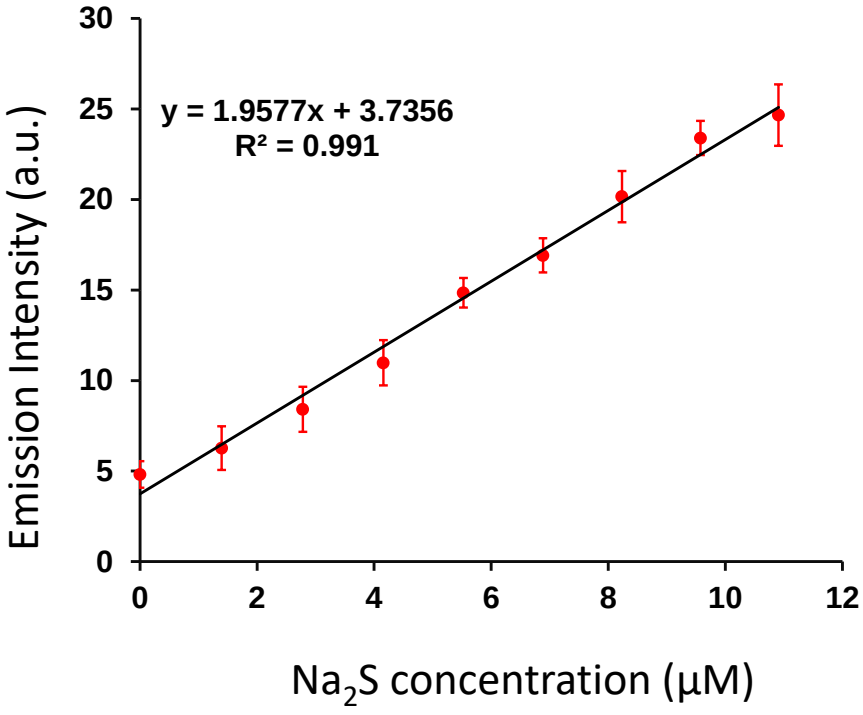

Figure S28: Liner turn-on response of **APBI-Cu** nanorods in presence of Na_2S.

Table S1: List of few recently reported sulfide sensor material works with similar metal ion displacement mechanism.

Sensor material	Sensing medium	Both Fluorometric and colorimetric	Involvement of organic solvent	Detection limit	Reference
Lipid bilayer vesicle embedded copper complex (Ves-1.Cu)	Phosphate buffer,	Yes	NO	4.06 μM	[1]
Azine based fluorescein indicator	HEPES–CH_3CN	NO	Yes	1.7 μM	[2]
Macrocyclic ring with naphthalimide moiety	H_2O–CH_3OH	Yes	Yes	0.7 μM	[3]
Cyanine NIR dye	aqueous solution with 1% DMSO	Yes	Yes	1.186 μM	[4]
Histidine-modified perylene diimide fluorescent probe	HEPES buffer	No	NO	0.41 μM	[5]
[Cu(MaT-cyclen)2]	water	NO	NO	0.205 μM	[6]
Zinc based Schiff base complex	CH_3CH_2OH–Tris–HCl buffer	NO	Yes	10^{-6} M	[7]
Coumarin-based fluorescent probe	HEPES buffer solution with 0.5% DMSO	NO	Yes	88.5 nM	[8]
BODIPY-based fluorescent probe	HEPES buffer with 5% CH_3CN	NO	Yes	5.5 μM.	[9]
Eu3+/Cu2+@Znpda MOF	HEPES buffer	NO	NO	1.45 μM	[10]
Eu(III)–Cu(II) Heterometallic–Organic Framework	HEPES buffer	NO	NO	0.130 μM	[11]

Diaminomaleonitrile (DAMN)-based salen-type zinc complex	DMSO	Yes	Yes	10 μM	[12]
lanthanide coordination polymer (AMP/Tb/Ag CP)	HEPES buffer	NO	NO	0.3 μM	[13]
Cyclam-functionalized CD/Cu2+	HEPES buffer	NO	NO	0.13 μM	[14]
Calix[4]arene benzothiazole/Cu2+	phosphate buffer	NO	NO	1.54 μM	[15]
carbon dots/Hg2+	HEPES buffer	NO	NO	0.32 μM	[16]
L-Cu2+ complex	HEPES buffer with 3% DMSO	NO	Yes	0.85 μM	[17]
Zinc Complex	CH_3CN–Tris-HCl buffer	NO	Yes	1.2 μM	[18]
Fluorescent probe (D-CN)	PBS buffer with 30% DMF	NO	Yes	30 μM.	[19]
APBI-Cu nanorods	pure Water and HEPES buffer	**YES**	**NO**	**0.181 μM**	**This Work**

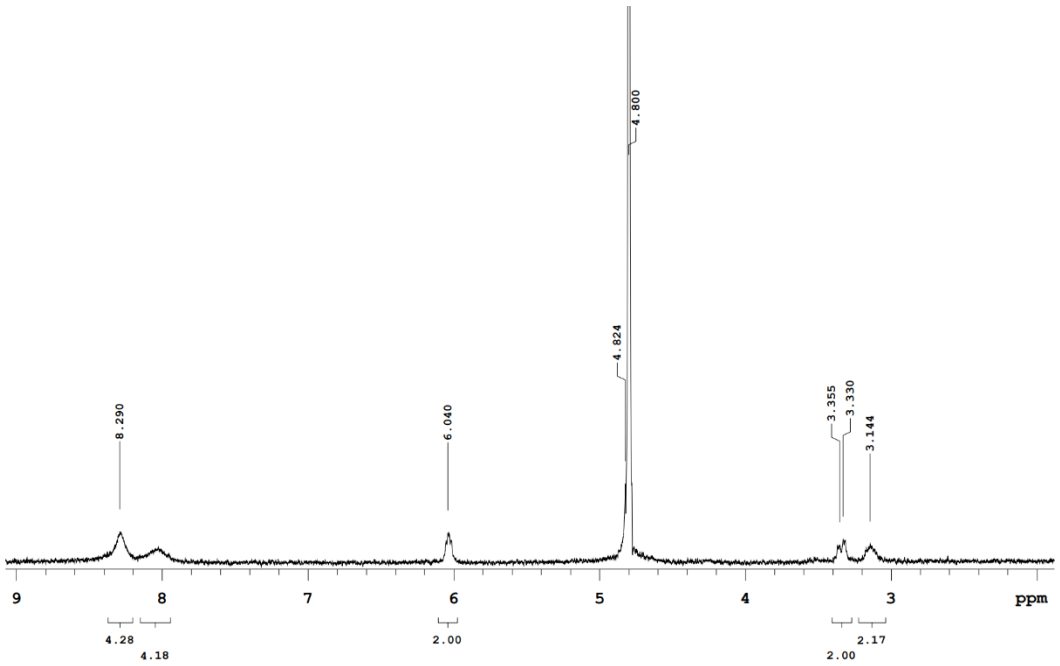

Figure S29: ^{1}H NMR spectra of APBI-K in D_2O.

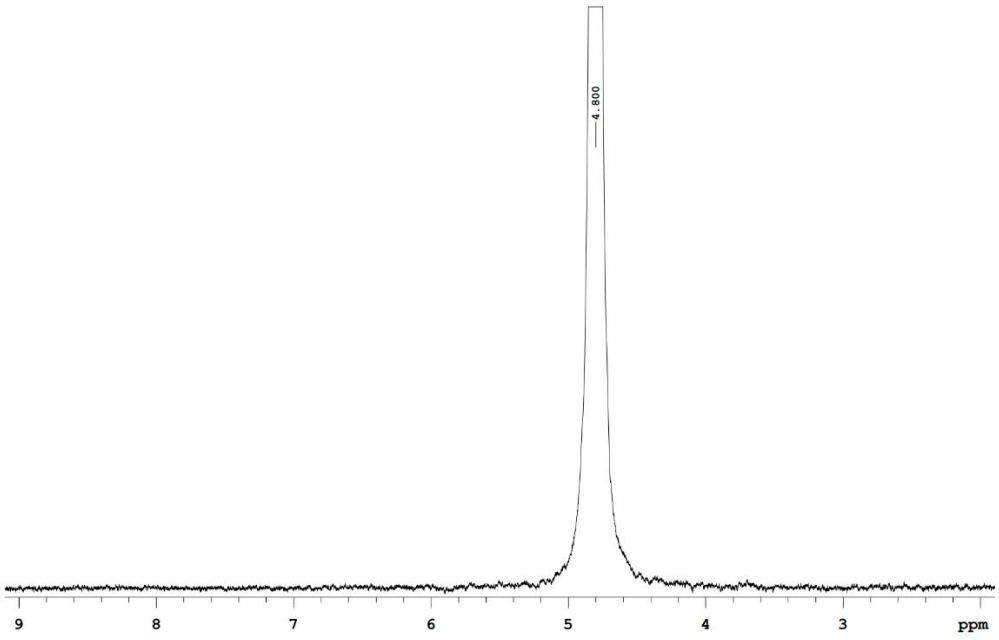

Figure S30: ^{1}H NMR spectra of APBI-K after complexation with Cu^{2+} ion in D_2O.

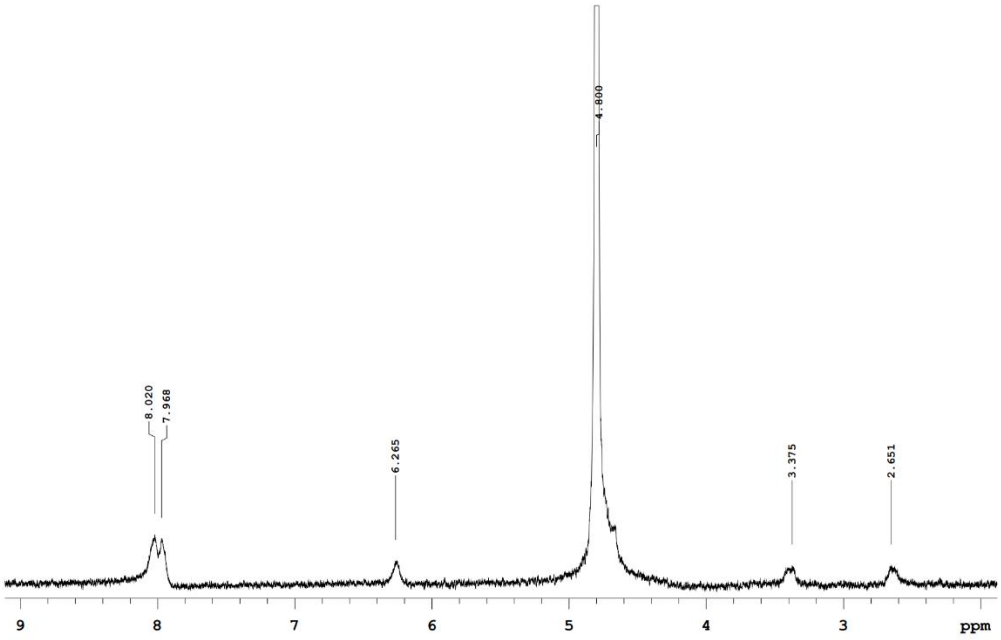

Figure S31: ^{1}H NMR spectra of **APBI-Cu** nanorods after treatment of Na_2S in D_2O.

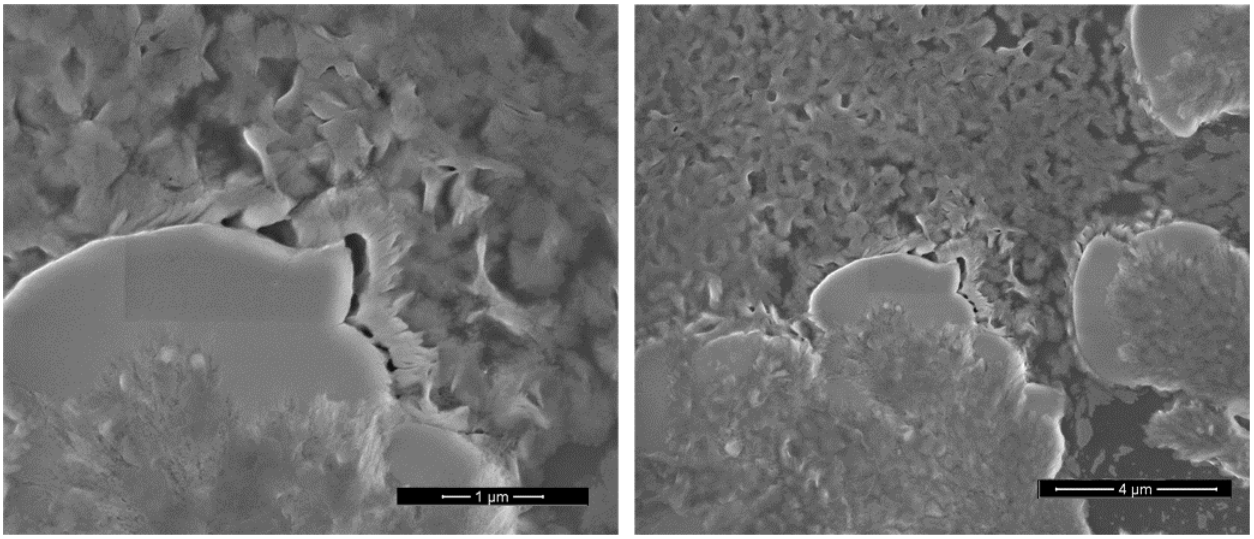

Figure S32: SEM images of **APBI-Cu** nanorods after the treatment of Na_2S.

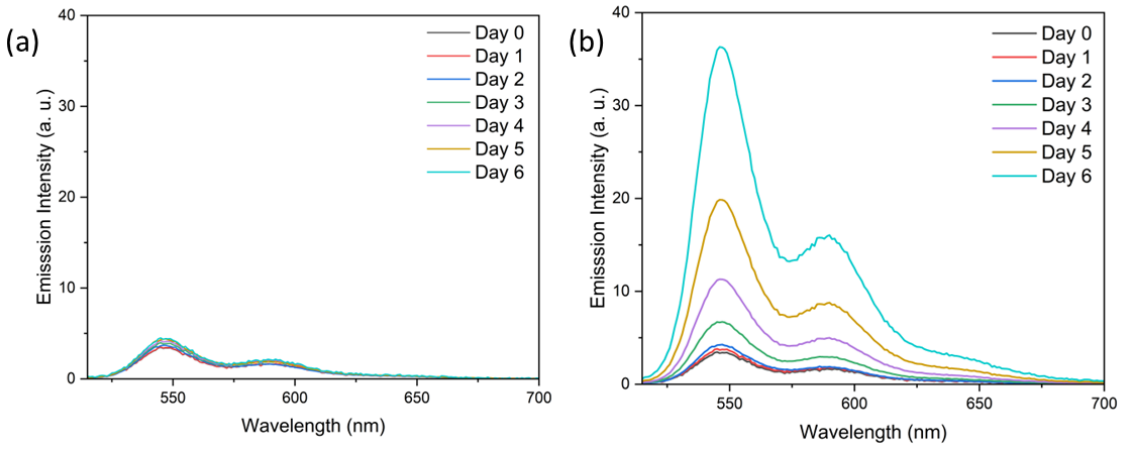

Figure S33: Change in emission spectra of **APBI-Cu** nanorods after bubbling the gas collected from meat sample stored at (a) -4 °C and (b) room temperature.

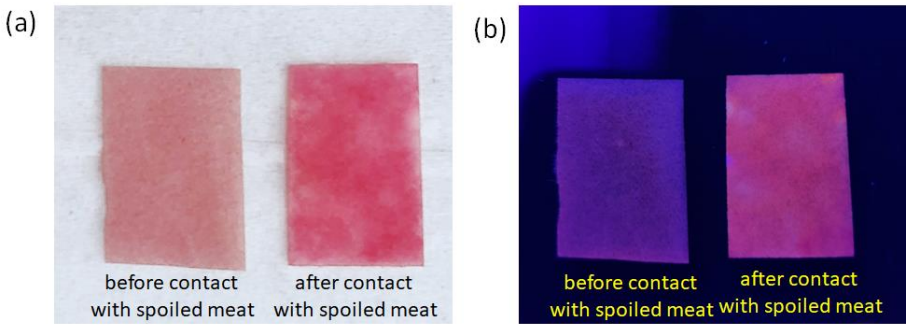

Figure S34. Digital images of paper strips coated with APBI-Cu under (a) daylight and (b) UV-lamp before and after the contact with spoiled meat.

References:

1. Kaushik, R.; Sakla, R.; Ghosh, A.; Selvan, G.T.; Selvakumar, P.M.; Jose, D.A. Selective detection of H2S by copper complex embedded in vesicles through metal indicator displacement approach. *ACS Sens.* **2018**, *3*, 1142-1148, doi:https://doi.org/10.1021/acssensors.8b00174.
2. Hou, F.; Cheng, J.; Xi, P.; Chen, F.; Huang, L.; Xie, G.; Shi, Y.; Liu, H.; Bai, D.; Zeng, Z. Recognition of copper and hydrogen sulfide in vitro using a fluorescein derivative indicator. *Dalton Trans.* **2012**, *41*, 5799-5804, doi:https://doi.org/10.1039/C2DT12462A.
3. Lou, X.; Mu, H.; Gong, R.; Fu, E.; Qin, J.; Li, Z. Displacement method to develop highly sensitive and selective dual chemosensor towards sulfide anion. *Analyst* **2011**, *136*, 684-687, doi:https://doi.org/10.1039/C0AN00742K.

4. Hu, Y.; Yin, J.; Yoon, J. A multi-responsive cyanine-based colorimetric chemosensor containing dipicolylamine moieties for the detection of Zn (II) and Cu (II) ions. *Sens. Actuators, B* **2016**, *230*, 40-45, doi:https://doi.org/10.1016/j.snb.2016.02.040.
5. Gao, X.; Li, Y.; Zhang, J.; Cheng, N.; Zhang, L.; Zhang, Z.; Yao, Z. Rapid detection of hydrogen sulfide in vegetables and monosodium glutamate based on perylene supramolecular aggregates using an indicator displacement assays strategy. *Spectrochim. Acta, Part A* **2022**, *276*, 121223, doi:https://doi.org/10.1016/j.saa.2022.121223.
6. Palanisamy, S.; Lee, L.-Y.; Wang, Y.-L.; Chen, Y.-J.; Chen, C.-Y.; Wang, Y.-M. A water soluble and fast response fluorescent turn-on copper complex probe for H2S detection in zebra fish. *Talanta* **2016**, *147*, 445-452, doi:https://doi.org/10.1016/j.talanta.2015.10.019.
7. Dong, Z.; Le, X.; Zhou, P.; Dong, C.; Ma, J. Sequential recognition of zinc ion and hydrogen sulfide by a new quinoline derivative with logic gate behavior. *RSC Adv.* **2014**, *4*, 18270-18277, doi:https://doi.org/10.1039/C3RA47755J.
8. Gao, L.-L.; Wang, B.-B.; Chen, X.; Wang, Y.; Wu, W.-N.; Zhao, X.-L.; Yan, L.-L.; Fan, Y.-C.; Xu, Z.-H. Hydrazone derivative bearing coumarin for the relay detection of Cu2+ and H2S in an almost neat aqueous solution and bioimaging in lysosomes. *Spectrochim. Acta, Part A* **2021**, *255*, 119693, doi:https://doi.org/10.1016/j.saa.2021.119693.
9. Wu, S.; Ma, X.; Wang, Y.; Zhou, J.; Li, X.; Wang, X. A novel fluorescent BODIPY-based probe for detection of Cu2+ and H2S based on displacement approach. *Spectrochim. Acta, Part A* **2021**, *249*, 119330, doi:https://doi.org/10.1016/j.saa.2020.119330.
10. Han, X.; Gu, C.; Ding, Y.; Yu, J.; Li, K.; Zhao, D.; Chen, B. Stable Eu3+/Cu2+-functionalized supramolecular Zinc (II) complexes as fluorescent probes for turn-on and ratiometric detection of hydrogen sulfide. *ACS Appl. Mater. Interfaces* **2021**, *13*, 20371-20379, doi:https://doi.org/10.1021/acsami.1c04013.
11. Zheng, X.; Fan, R.; Song, Y.; Xing, K.; Wang, P.; Yang, Y. Dual-Emitting Eu (III)–Cu (II) heterometallic–organic framework: simultaneous, selective, and sensitive detection of hydrogen sulfide and ascorbic acid in a wide range. *ACS Appl. Mater. Interfaces* **2018**, *10*, 32698-32706, doi:https://doi.org/10.1021/acsami.8b11367.
12. Strianese, M.; Guarnieri, D.; Lamberti, M.; Landi, A.; Peluso, A.; Pellecchia, C. Fluorescent salen-type Zn (II) complexes as probes for detecting hydrogen sulfide and its anion: Bioimaging applications. *Inorg. Chem.* **2020**, *59*, 15977-15986, doi:https://doi.org/10.1021/acs.inorgchem.0c02499.
13. Liu, B.; Chen, Y. Responsive lanthanide coordination polymer for hydrogen sulfide. *Anal. Chem.* **2013**, *85*, 11020-11025, doi:https://doi.org/10.1021/ac402651y.
14. Chen, J.; Li, Y.; Lv, K.; Zhong, W.; Wang, H.; Wu, Z.; Yi, P.; Jiang, J. Cyclam-functionalized carbon dots sensor for sensitive and selective detection of copper (II) ion and sulfide anion in aqueous media and its imaging in live cells. *Sens. Actuators, B* **2016**, *224*, 298-306, doi:https://doi.org/10.1016/j.snb.2015.10.046.
15. Wang, Z.-X.; Zheng, C.-L.; Ding, S.-N. Label-free detection of sulfide ions based on fluorescence quenching of unmodified core–shell Au@ Ag nanoclusters. *RSC adv.* **2014**, *4*, 9825-9829, doi:https://doi.org/10.1039/C3RA45019H.

16. Barati, A.; Shamsipur, M.; Abdollahi, H. Metal-ion-mediated fluorescent carbon dots for indirect detection of sulfide ions. *Sens. Actuators, B* **2016**, *230*, 289-297, doi:https://doi.org/10.1016/j.snb.2016.02.075
17. Hai, Z.; Bao, Y.; Miao, Q.; Yi, X.; Liang, G. Pyridine–biquinoline–metal complexes for sensing pyrophosphate and hydrogen sulfide in aqueous buffer and in cells. *Anal. Chem.* **2015**, *87*, 2678-2684, doi:https://doi.org/10.1021/ac504536q.
18. Dong, Z.; Le, X.; Zhou, P.; Dong, C.; Ma, J. An "off–on–off" fluorescent probe for the sequential detection of Zn 2+ and hydrogen sulfide in aqueous solution. *New J. Chem.* **2014**, *38*, 1802-1808, doi:https://doi.org/10.1039/C3NJ01487H.
19. Ren, M.; Xu, Q.; Bai, Y.; Wang, S.; Kong, F. Construction of a dual-response fluorescent probe for copper (II) ions and hydrogen sulfide (H2S) detection in cells and its application in exploring the increased copper-dependent cytotoxicity in present of H2S. *Spectrochim. Acta, Part A* **2021**, *249*, 119299, doi:https://doi.org/10.1016/j.saa.2020.119299.